IEEE Access
Multidisciplinary | Rapid Review | Open Access Journal

Received January 9, 2019, accepted January 23, 2019, date of publication February 4, 2019, date of current version February 27, 2019.

Digital Object Identifier 10.1109/ACCESS.2019.2895821

Dynamic Sliding Mode Control of Active Power Filter With Integral Switching Gain

YUN CHEN AND JUNTAO FEI

Jiangsu Key Laboratory of Power Transmission and Distribution Equipment Technology, College of IoT Engineering, Hohai University, Changzhou 213022, China

Corresponding author: Juntao Fei (jtfei@hhu.edu.cn)

This work was supported in part by the National Science Foundation of China under Grant 61873085, in part by the Natural Science Foundation of Jiangsu Province under Grant BK20171198, and in part by the Fundamental Research Funds for the Central Universities under Grant 2017B20014 and Grant 2017B21214.

ABSTRACT Owing to the fact that the active power filter with conventional sliding mode controller has a chattering problem, an improved dynamic sliding mode controller is proposed in this paper to increase the performance of the APF. A dynamic sliding mode controller with integral switching gain is developed. The first-order dynamic sliding surface has the characteristic of transferring the discontinuity in traditional sliding mode control to the first derivative of the controller. Therefore, a continuously dynamic sliding controller can be obtained, so that it can effectively weaken the chattering. In the meantime, the appropriate selection of switching gain can also reduce chattering. The simulation results show that the proposed control strategy possesses good performance to suppress the harmonics. Moreover, the hardware in the loop experiment proves the practicability of the proposed algorithm.

INDEX TERMS Dynamic sliding mode control, integral switching gain, hardware-in-the-loop, active power filter.

I. INTRODUCTION

Development of power technology has brought variety of benefits to our lives. On the one hand, with the proliferation of nonlinear loads of power electronic device in electric power distribution system such as Uninterruptible Power Supply (UPS), Personal Computer (PC), Compact Fluorescent Lamp (CFL), current harmonic pollution at the grid side is growing. On the other hand, the widespread use of large-capacity inductive devices such as motors and transformers will result in a reduction in the power factor. The existence of harmonic current will reduce power quality and increase line loss, with the constant superposition of harmonic current, the communication quality of sensitive device near to the harmonic source will be impacted, some sensitive equipment may cause malfunction due to harmonic current, even giving rise to security issue [1]. The reduction of power factor will lead to the decrease of electricity efficiency and voltage, and even lead to the collapse of the power grid. These problems will seriously influence the normal operation of the power grid system and cause economic losses.

The associate editor coordinating the review of this manuscript and approving it for publication was Ligang Wu.

With more and more high-precision equipment in industry, the power grid with harmonic and reactive power problems cannot meet the requirements. Therefore, how to improve the quality of power grids and eliminate the harm of harmonic current will inevitably become a hot research topic in society.

Up to now, passive filters widely installed in the industry are used to decrease harmonic current in power system, they consist of a capacitor and an inductor. However, passive filters have many imperfections, such as just injecting fixed frequency harmonic current and a small installed capacity, so they can not achieve a good compensation performance. Ultimately, traditional passive filters will be gradually replaced by active power filter s(APF) [2]–[7]. APFs are a new type of compensation equipments, the principle of active power filters is to improve power quality by injecting compensating harmonic current whose amplitude is equal to the reference current, but the phase is opposite.

APF have many different structures. According to the grid connection method, there are series and parallel structures. Parallel structure adopts a coupling transformer to connect to the grid, there is no harmful effect for the grid system. According to the difference of DC side energy storage components, there are voltage and current structures.

The advantages of the voltage structure include lower losses, higher efficiency, and easy to expansion. There are single and three phases based on classification by phase. Single-phase structure is only suitable for low power applications. This paper will take three phase APF which is a voltage parallel structure as the research object.

The selection of control strategy for active power filter is the key to achieve better compensation effect. Traditional control strategy includes hysteresis control, space vector control and triangle carrier wave control. Harshithananda *et al.* [8] designed a hysteresis control technique of VSI to reduce harmonics of active power filter. Yang *et al.* [9] proposed a 3-D space vector PWM for three-phase four-wire active filter. Tang and Liao [10] designed a shunt hybrid active power filter based on PSCAD/EMTDC. It is shown that traditional control strategy can not maximize compensation performance of active power filter [8]–[10]. Therefore, it is necessary to choose an advanced controller to replace the tradition control for active power filter.

Sliding mode control (SMC) is a variable structure control which is insensitive to parameter changes and uncertain disturbance. Liu *et al.* [11] design an extended State Observer-Based Sliding-Mode Control for Three- Phase Power Converters. Liu *et al.* [12] proposed an observer-based higher order sliding mode control of power factor in three-phase AC/DC converter for hybrid electric vehicle applications. In the above literatures, a sliding mode controller for power electronic converters has been successfully designed., this provides guidance for applying sliding mode control to active power filters.

The main circuit of the active power filter is composed of six switching inverters and dc side capacitor. When the state of the converter in the main circuit changes, its topology will also change. Thus, SMC can exhibit a better control performance than other control strategy in the active power filter which is a variable structure device. Saetieo *et al.* [13] design a three-phase active power filter based on sliding mode control. Battista and Mantz [14] proposed a harmonic series compensator with sliding mode in power systems. Zhu *et al.* [15] designed a sliding mode control with variable structure of series active power filter. Yarahmadi *et al.* [16] proposed a current harmonics reduction of non-linear load by using active power filter based on improved sliding mode control. Neural network controllers have been combined with sliding mode control to improve the performance of the APF in [17]–[19]. The above literatures have successfully applied sliding mode control to active power filters, experimental results shown that the active power filter can compensate harmonic current. In the future study of active power filters, the combination of multiple intelligent control is a development trend. The literatures [20]–[22] provide some research ideas, and it is expected to further improve the control performance of sliding mode control in APF.

However, inherent chattering phenomenon in sliding mode control always exists. Jeong and Woo [23] used DSP to verify the practicality and reliability of the algorithm, but DSP processing speed is limited, it can not implement too complex control algorithm. Compared with DSP, dSPACE [24]–[26] can seamlessly link to MATLAB and has faster calculation speeds. Thus, this paper uses dSPACE instead of DSP to verify algorithm performance. A dynamic sliding mode controller with integral switching gain is designed. The experimental results show that the proposed algorithm can quickly compensate harmonic current and effectively suppress chattering. The main contributions of this paper compared with existing works can be emphasized as follows:

(1) This paper combines the advantages of dynamic sliding surface and switching gain. Dynamic sliding mode control is to design a new sliding surface that is related to the first derivative of the input, it eliminates chattering by transferring discontinues item to the first derivative of control. Meanwhile, the appropriate selection of switching gain can also effectively suppress the chattering.

(2) In order to better display the superiority of sliding mode control and shorten the development cycle. This paper uses dSPACE platform to design APF prototype. The MATLAB simulation and experiment results shows that the improved sliding control strategy endow excellent dynamic characteristics and achieve very low total harmonic distortion (THD).

This paper is organized as follows. In section II, the dynamics of active power filter is introduced. In section III, a traditional sliding mode controller is introduced. In section IV, dynamic sliding mode control using integral switching gain is proposed to guarantee the stability of the closed loop system. In section V, simulation results comparing with traditional sliding mode control are presented. In section VI, the implementation of control algorithm based on ds1104 experiment platform is done. Finally, conclusions are provided in section VII.

II. MODELING OF THE ACTIVE POWER FILTER

Harmonic current mainly come from the industrial field. At same time, most of the equipment in the industry uses three-phase source. Thus, the three-phase shunt APF is selected as the research object in this paper, its topology diagram is shown in Fig. 1.

In the Fig. 1, v_i $(i = a, b, c)$ is the connection point voltage, $u_{iN}(i = a, b, c)$ is the AC side voltage of APF to ground. $i_{li}(i = a, b, c)$ is the load current, $i_{ci}(i = a, b, c)$ is the compensation current. In addition, R and L are the resistance and inductance of the active power filter respectively, U_{dc} is the DC side voltage, $v_{NN'}$ is the voltage between point N and N'. According to *Kirchhoff's* theorem, the following dynamic equation can be obtained:

$$\begin{cases} v_a - u_{aN'} + u_{NN'} = L\dfrac{di_{ca}}{dt} + Ri_{ca} \\ v_b - u_{bN'} + u_{NN'} = L\dfrac{di_{cb}}{dt} + Ri_{cb} \\ v_c - u_{cN'} + u_{NN'} = L\dfrac{di_{cc}}{dt} + Ri_{cc} \end{cases} \tag{1}$$

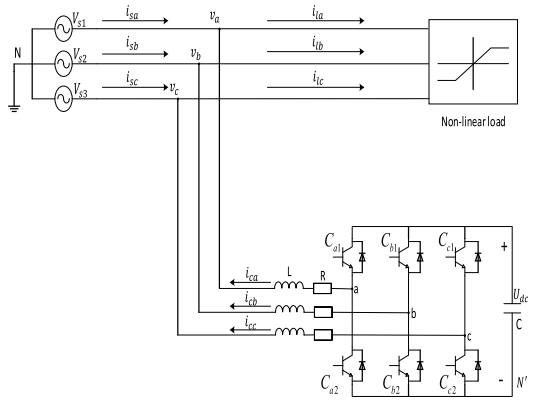

FIGURE 1. The topology diagram of active power filter.

Assume IGBT is an ideal device, using the switching function to express the working state of the IGBT. Thus, we can define the following expression:

$$S_i = \begin{cases} 1, & if\ c_{i1}\ is\ on\ and\ c_{i2}\ is\ off \\ 0, & if\ c_{i1}\ is\ off\ and\ c_{i2}\ is\ on \end{cases} \tag{2}$$

where $i = a, b, c$.

AC side output voltage can be established by the switching function:

$$\begin{cases} u_{aN'} = S_a U_{dc} \\ u_{bN'} = S_b U_{dc} \\ u_{cN'} = S_c U_{dc} \end{cases} \tag{3}$$

Substituting (3) into (1) yields:

$$\begin{cases} \dfrac{di_{ca}}{dt} = -\dfrac{R}{L} i_{ca} - \dfrac{U_{dc}}{L} S_a + \dfrac{1}{L} u_{NN'} + \dfrac{1}{L} v_a \\ \dfrac{di_{cb}}{dt} = -\dfrac{R}{L} i_{cb} - \dfrac{U_{dc}}{L} S_b + \dfrac{1}{L} u_{NN'} + \dfrac{1}{L} v_b \\ \dfrac{di_{cc}}{dt} = -\dfrac{R}{L} i_{cc} - \dfrac{U_{dc}}{L} S_c + \dfrac{1}{L} u_{NN'} + \dfrac{1}{L} v_c \end{cases} \tag{4}$$

Equation (4) is established in the *abc* stationary coordinate system. Although there are no couplings among the three-phase equations, the design of control system is slightly complicated. Thus, use a transformational matrix between the *abc* stationary coordinate system and $\alpha\beta$ stationary coordinate system to simplify the Eq. (4). The transformational matrix can be expressed as follows:

$$\begin{bmatrix} x_\alpha \\ x_\beta \end{bmatrix} = C_{3/2} \begin{bmatrix} x_a \\ x_b \\ x_c \end{bmatrix}, C_{3/2} = \sqrt{\frac{2}{3}} \begin{bmatrix} 1 & -\frac{1}{2} & -\frac{1}{2} \\ 0 & \frac{\sqrt{3}}{2} & -\frac{\sqrt{3}}{2} \end{bmatrix} \tag{5}$$

$$\begin{bmatrix} x_a \\ x_b \\ x_c \end{bmatrix} = C_{2/3} \begin{bmatrix} x_\alpha \\ x_\beta \end{bmatrix}, \quad C_{2/3} = \begin{bmatrix} 1 & 0 \\ -\frac{1}{2} & \frac{\sqrt{3}}{2} \\ -\frac{1}{2} & -\frac{\sqrt{3}}{2} \end{bmatrix} \tag{6}$$

Rewrite (4) as a matrix expression as:

$$\begin{bmatrix} \dfrac{di_{ca}}{dt} \\ \dfrac{di_{cb}}{dt} \\ \dfrac{di_{cc}}{dt} \end{bmatrix} = -\frac{R}{L} \begin{bmatrix} i_{ca} \\ i_{cb} \\ i_{cc} \end{bmatrix} - \frac{U_{dc}}{L} \begin{bmatrix} S_a \\ S_b \\ S_c \end{bmatrix} + \frac{1}{L} \begin{bmatrix} u_{NN'} \\ u_{NN'} \\ u_{NN'} \end{bmatrix} + \frac{1}{L} \begin{bmatrix} v_a \\ v_b \\ v_c \end{bmatrix} \tag{7}$$

Multiply (4) by the transformational matrix $C_{3/2}$

$$\begin{bmatrix} \dfrac{di_\alpha}{dt} \\ \dfrac{di_\beta}{dt} \end{bmatrix} = -\frac{R}{L} \begin{bmatrix} i_\alpha \\ i_\beta \end{bmatrix} + \frac{1}{L} \begin{bmatrix} v_\alpha \\ v_\beta \end{bmatrix} - \frac{U_{dc}}{L} \begin{bmatrix} S_\alpha \\ S_\beta \end{bmatrix} \tag{8}$$

The simplified equation (8) does not have couplings and looks simpler. The working principle of active power filter can be described as: The current sensor measures load current in real-time, then utilizes the FFT algorithm to calculate the reference current, PWM signals which is used to control IGBT on and off is generated by the control strategy. Finally, the AC side of the active power filter generates the compensation current whose amplitude is equal to the reference current, but the phase is opposite. When the compensation current is injected into the grid, the purpose of suppressing harmonics can be achieved. The above working principle is shown in Fig. 2.

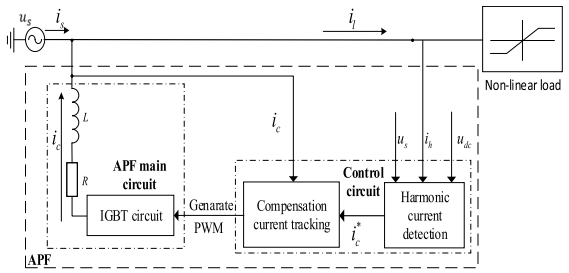

FIGURE 2. The working principle diagram of APF.

Considering the model uncertainties and external disturbances, the model of the APF can be transformed as:

$$\dot{x} = f(x) - bu + d \tag{9}$$

where $x = \begin{bmatrix} i_\alpha & i_\beta \end{bmatrix}^T, f(x) = -\frac{R}{L} i_k + \frac{1}{L} v_k, k = \alpha, \beta$. $b = \frac{U_{dc}}{L}, u = \begin{bmatrix} S_\alpha & S_\beta \end{bmatrix}^T$, d is the model uncertainties and external disturbances bounded by $|d| < D_0$, where D_0 is a positive constant.

It can be seen from the above working principle: the first thing is to extract harmonic current. If the detected harmonic current is inaccurate or there is a high delay, the compensation current output by the controller will also have errors and high delays. When the compensation current is connected to the grid, the grid current will not be converted to sine wave. Therefore, the extraction of harmonic current has great influence on the performance of APF. This paper adopts a fast harmonic detection method ($p - q$) based on instantaneous

reactive power theory. Assuming the load is three-phase symmetrical, the grid only contains positive sequence current, the principle of harmonic detection is shown in Fig. 3.

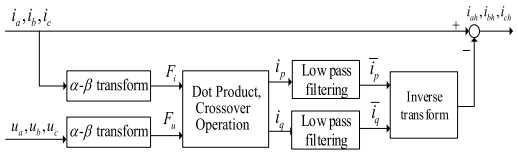

FIGURE 3. $p-q$ harmonic detection principle.

The dot product and crossover operation results represent the current component on the $p-q$ coordinate axis, where i_p is the active current and i_q is the reactive current.

III. TRADITIONAL SLIDING MODE CONTROLLER

The aim of the sliding mode controller is to allow the compensation current to rapidly and accurately track the reference current.

Consider the following nonlinear system:

$$\dot{x} = f(x) - bu + d \tag{10}$$

where $b > 0, x \in R^n, u \in R, |d| < D_0$, where D_0 is a positive constant.

Define error as:

$$e = r - x \tag{11}$$

where r is the reference current, and x is the compensation current. Then the conventional sliding surfaces can be defined as follows:

$$S = ce \tag{12}$$

Where c is a 2-dimensional diagonal matrix and nonsingular matrix. The existence of c needs to ensure that the sliding surfaces S is stable. We ignore uncertain disturbance, and define $\dot{S} = 0$,

$$\begin{aligned} \dot{S} &= c\dot{e} \\ &= c\left(\dot{r} - \dot{x}\right) \\ &= c\dot{r} - c\left(f(x) - bu\right) = 0 \end{aligned} \tag{13}$$

Solving Equation (13), the equivalent control can be obtained as:

$$u_{eq} = [bc]^{-1}(cf(x) - c\dot{r}) \tag{14}$$

However, real system has unknown model uncertainties and external disturbances. According to the theory of sliding mode control, when the system state point is not on the switching surface, the switching function plays a leading role in the system, which ensures that the system state point reaches the sliding mode surface within a limited time. When the state point reaches the sliding surface, we want the system state point to maintain motion on the switching surface, now, the equivalent control dominates in the system.

When the system state point goes to the switching surface, the system state point cannot be stopped immediately at the switching surface because there is a system inertia. Because of switching control, the system state point will fluctuate near the switching surface, which is the main cause of the control error. If the switching function is too small, it takes too long for the system state point to reach the switching surface; if it is too large, there is a large chattering and error. Reasonable selection of the switching function will help to reduce the error of the system.

In order to meet the sliding mode arrival conditions $S\dot{S} \le -\eta|S|$, the traditional switching control is selected:

$$u_{sw} = -[bc]^{-1}K\,\mathrm{sgn}(S), \quad K > 0 \tag{15}$$

The switching control term in Eq. (15) is used to compensate for unknown uncertainties and disturbances in the system.

Finally, the total controller can be designed as:

$$\begin{aligned} u &= u_{eq} + u_{sw} \\ &= [bc]^{-1}(cf(x) - c\dot{r} - K\,\mathrm{sgn}(S)) \end{aligned} \tag{16}$$

Define Lyapunov function:

$$V = \frac{1}{2}S^T S = \frac{1}{2}\left(S_1^2 + S_2^2\right) > 0 \tag{17}$$

Stability analysis can be acquired from (10), (16), (17). The derivative of Eq. (17) becomes:

$$\begin{aligned} \dot{V} &= \frac{1}{2}S^T\dot{S} + \frac{1}{2}\dot{S}^T S = S^T\dot{S} \\ &= S^T[c(\dot{r} - \dot{x})] \\ &= S^T[c\dot{r} - c(f(x) - bu)] \\ &= S^T\left\{c\dot{r} - cf(x) + bc\left[(bc)^{-1}(cf(x) - c\dot{r} - K\,\mathrm{sgn}(s)\right]\right\} \\ &= S^T\left(-K\,\mathrm{sgn}(s)\right) \\ &= -K(|S_1| + |S_2|) \end{aligned} \tag{18}$$

Because of $K > 0$, $\dot{V} = S^T\dot{S} < 0$. Thus, conventional sliding mode controller can guarantee the stability of the APF system.

IV. IMPROVED SLIDING MODE CONTROLLER

In section III, we introduced how to design a conventional sliding mode controller. However, traditional sliding mode controller easily causes chattering, a dynamic sliding mode controller with integral switching gain is proposed. The structure of dynamic sliding mode control using integral switching gain is shown in Fig. 4.

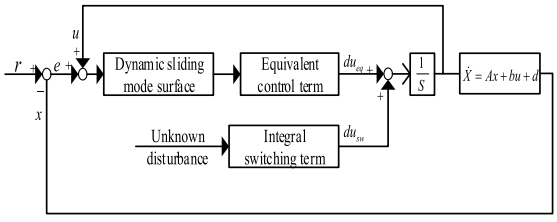

FIGURE 4. The structure of the proposed sliding mode controller.

Define instruction reference current $r = \left[i_\alpha^* \; i_\beta^* \right]^T$, the error can be defined as follows:

$$e = r - x \tag{19}$$

The first derivative of the error is:

$$\dot{e} = \dot{r} - \dot{x} \tag{20}$$

In order to better eliminate the chattering, we can modify the traditional sliding surface. Based on the traditional sliding surface, consider adding a polynomial that is related to the controller input. Its purpose is to convert the discontinuity of the system state into the first derivative of the controller. Therefore, we can get the following dynamic sliding surface:

$$S = ce + Du \tag{21}$$

where c is a 2-dimensional diagonal matrix and nonsingular matrix. $D > 0$ is a scalar. When reaching the sliding surface $S = 0$, $Du = -ce$. In order to form negative feedback, we require that the diagonal element of matrix c to be less than zero.

The first derivative of S becomes:

$$\dot{S} = c\dot{e} + D\dot{u} \tag{22}$$

Define $\dot{S} = 0$ to obtain equivalent control:

$$\dot{u}_{eq} = -\frac{1}{D}(c(\dot{r} - \dot{x})) \tag{23}$$

According to the traditional sliding mode control theory. In order to make the system reach the switching surface quickly and eliminate the uncertainty error and disturbance, we need to select an appropriate switching function.

Although the traditional switching function can ensure system stability, it is easy to cause chattering and error. Based on equation (15), we add an additional gain term that includes the integral of the switching surface. Get the following switch function:

$$\dot{u}_{sw} = -\frac{1}{D}K_w K_\rho \mathrm{sgn}(s), \quad K_w > 0 \tag{24}$$

where $K_\rho = \begin{bmatrix} \rho_1 & 0 \\ 0 & \rho_2 \end{bmatrix}$ is a diagonal matrix. And we define $\rho_i = \left| \int_0^t (K_f \rho_i + S_i) dt \right|$, $(i = 1, 2)$ and $K_f < 0$.

The proposed switching control has the following advantages: when the system state point is far away from the sliding mode surface, the switching gain is large, and the system state point will quickly approach the sliding mode surface. When the system state point approaches the sliding mode surface, the switching gain approaches 0, and the switching control is disabled. Finally, it can effectively eliminate the chattering.

Ultimately, the dynamic sliding mode controller is proposed as:

$$\begin{aligned} \dot{u} &= \dot{u}_{eq} + \dot{u}_{sw} \\ &= -\frac{1}{D}(c(\dot{r} - \dot{x})) - \frac{1}{D}K_w K_\rho \mathrm{sgn}(s)) \\ &= -\frac{1}{D}\left[c\dot{e} + K_w K_\rho \mathrm{sgn}(s)\right] \end{aligned} \tag{25}$$

where $K_\rho = \begin{bmatrix} \rho_1 & 0 \\ 0 & \rho_2 \end{bmatrix}$.

Choose a *Lyapunov*function as:

$$V = \frac{1}{2}S^T S = \frac{1}{2}\left(S_1^2 + S_2^2\right) > 0 \tag{26}$$

Then the first derivative of V becomes:

$$\begin{aligned} \dot{V} &= \frac{1}{2}S^T \dot{S} + \frac{1}{2}\dot{S}^T S = S^T \dot{S} \\ &= S^T \left[c(\dot{r} - \dot{x}) + D\dot{u}\right] \\ &= S^T \left\{ c\dot{e} + D\left\{ -\frac{1}{D}\left[c\dot{e} + K_w K_\rho \mathrm{sgn}(s)\right] \right\} \right\} \\ &= S^T \left\{ c\dot{e} - c\dot{e} - K_w K_\rho \mathrm{sgn}(s) \right\} \\ &= S^T \left(-K_w K_\rho \mathrm{sgn}(s) \right) \\ &= -K_w(\rho_1 |S_1| + \rho_2 |S_2|) \end{aligned} \tag{27}$$

where $\rho_i = \left| \int_0^t (K_f \rho_i + S_i) dt \right|$, $(i = 1, 2)$.

Because of $K_w > 0$ and $(\rho_1 |S_1| + \rho_2 |S_2|) > 0$, we can deduce $\dot{V} < 0$. It can be proved that the stability of control system can be guaranteed.

As can be seen from design of equation (25), the parameter K_w is used to eliminate unknown disturbances. At same time, the parameter K_w accounts for a large proportion when the controller is adjusted. Therefore, proper selection of K_w can effectively reduce tracking error.

V. SIMULATION STUDY

To verify the feasibility of the proposed algorithm, MATLAB/SIMULINK simulation is implemented. The DC side voltage control also needs to be considered during the simulation. When the APF is working normally, there is energy exchange between the DC side capacitor and the grid. This will cause fluctuations in the DC side voltage. The fluctuation of the DC side voltage will affect the APF compensation effect. In order to ensure that APF can provide constant harmonic compensation current to the grid system, we need to make ensure that the DC side voltage is a fixed value. This paper uses a traditional PI controller to regulate the DC side voltage.

The line resistance, switching loss and AC side inductance of the active power filter consume a certain amount of active power. And the consumption of active power must cause the capacitor voltage on the DC side to decrease. Therefore, we can ensure that the DC side voltage is constant by compensating the active power.

Usually, the DC side voltage is subtracted from the reference voltage, the input of the PI controller is the obtained error, the output is the active current component to be compensated, and finally the output of the PI is added to the active current portion of the command reference current. The voltage control loop is shown in Fig. 5.

Due to the fact that the control speed of the voltage loop is about one tenth of the current tracking control speed, parameters K_p and K_I are relatively small, Properly increasing the

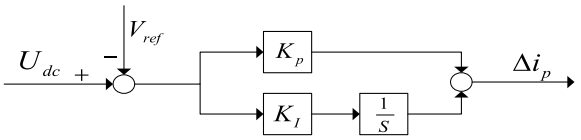

FIGURE 5. The DC side voltage control loop.

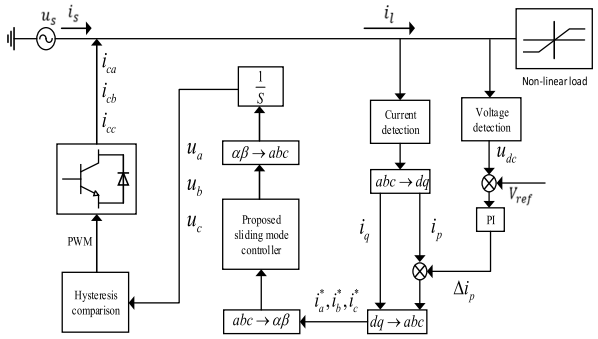

FIGURE 6. The control block diagram of active power filter.

parameter K_p can shorten the rise time, but it will increase overshoot.

After we combined current tracking control system as in Fig. 4 and voltage control system as in Fig. 5, we can obtain the control block diagram of active power filter as in Fig. 6. According to Fig. 6, we can build a simulation model. The simulation parameters are shown in Table 1.

TABLE 1. Active power filter model parameters.

Parameters	Values
Three-phase voltage	$220V_{rms}$ / $50Hz$
Non-linear loads	$R = 10\Omega$, $L = 5e^{-3}H$
Main circuit parameters	$R = 0.1\Omega$, $L = 0.01H$ $C = 5e^{-3}F$ $V_{ref} = 1KV$

During the simulation, active power filter starts to work in the time t = 0.04 s. Its means that the state before 0.04s represents the daily state of the grid, which may contain harmonics changing at any time. At the 0.04s, the prototype began to work, which includes detecting the harmonics in the current state grid and outputting harmonic compensation current. Then, in order to verify the dynamic property of the algorithm, adding an identical non-linear load in the time t = 0.25 s. From Fig. 7, load current is strictly distorted by non-linear load, from Fig. 8, we can see that the THD of the supply current is 24.71%. Thus, if we directly connect the load current to the power grid without taking any action, the quality of power grid can not be guaranteed.

As can be shown in Fig. 9, under the control of two control strategies, it can be clearly seen that the load current waveform is close to a sinusoidal waveform. Even if the non-linear load changes, the load current waveform can

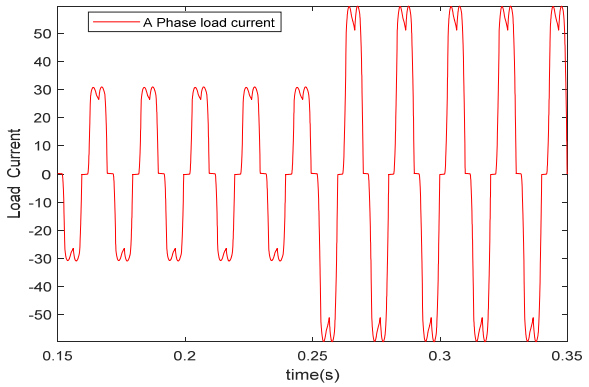

FIGURE 7. The grid current waveform without active power filter.

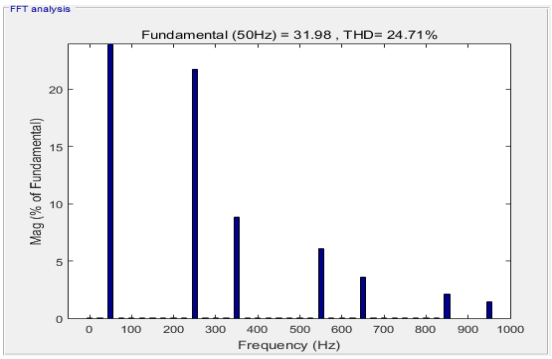

FIGURE 8. The total harmonic distortion without active power filter.

quickly approach the sinusoidal waveform. However, it is obvious that the load current waveform using proposed controller is smoother than the load current waveform using traditional controller.

Fig. 10 shows the DC-side voltage tracking waveform under two controls. The DC side voltage is controlled by traditional PI, and the control parameters are the same. The stability of the DC side voltage is the premise of harmonic current compensation. In the Fig. 10, although the DC side voltage control parameters are the same, the proposed harmonic current controller can make the DC side waveform more stable, and its fluctuation range is around 1000V, especially when the load changes. In fact, the small fluctuations in the DC-side voltage have little effect on the compensation performance of the active power filter.

TABLE 2. Thd using two different controllers at different times.

Methd / Time	Proposed controller	Traditional SMC
0s	24.71%	24.71%
0.15s	2.71%	3.67%
0.40s	1.75%	4.85%

Fig. 11 is the FFT analysis using two different controls at different times. Fig. 11(a) and Fig. 11(b) are the total

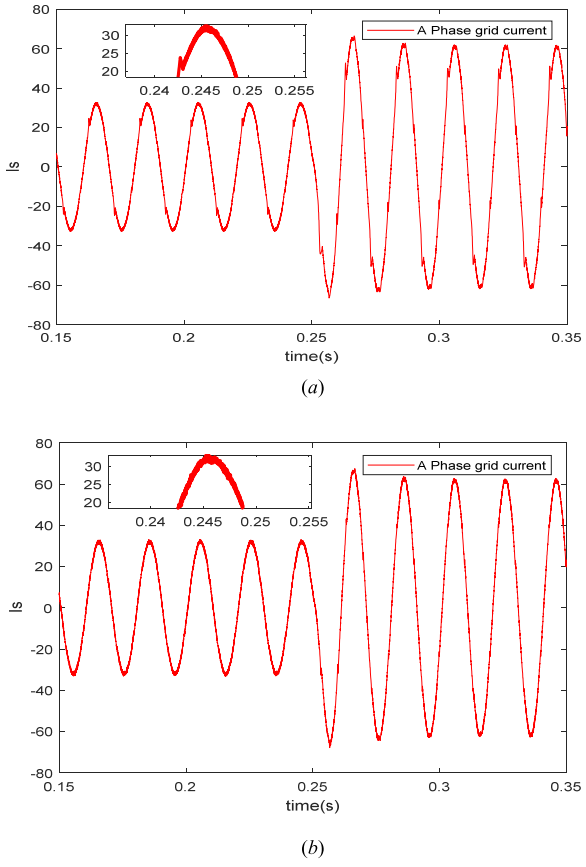

FIGURE 9. The grid current waveform (*a*) using traditional controller (*b*) using proposed controller.

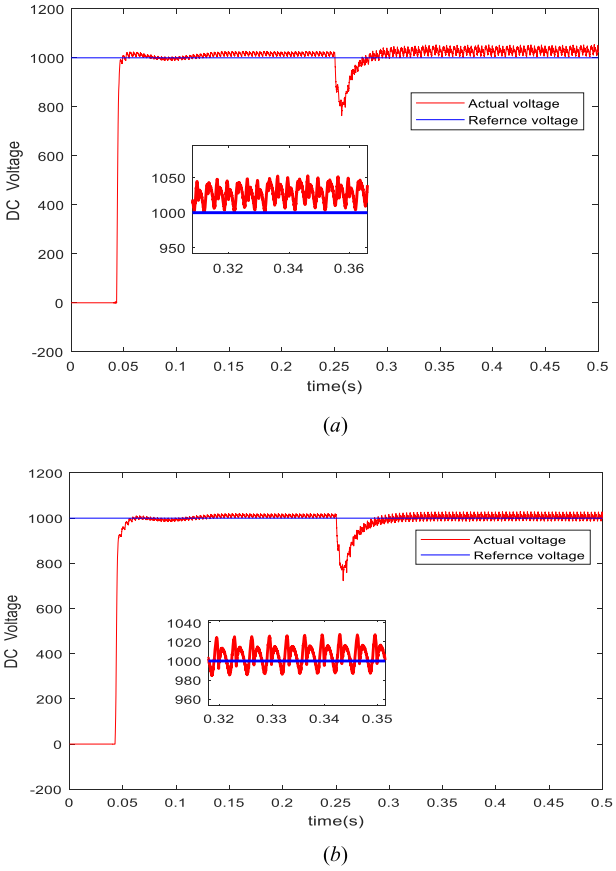

FIGURE 10. Actual voltage and reference voltage (*a*) using traditional controller (*b*) using proposed controller.

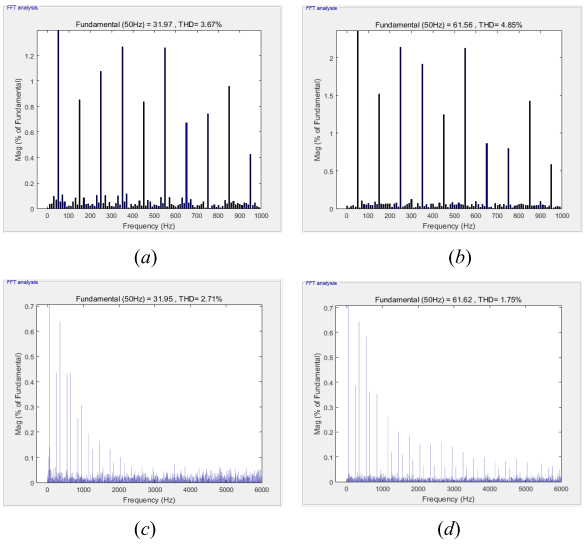

FIGURE 11. Total harmonic distortion using two different controllers.

harmonic distortion of the supply current using traditional controller at 0.15 s and 0.4 s respectively, Fig. 11(c) and Fig. 11(d) are the total harmonic distortion of the supply current using proposed controller at 0.15 s and 0.4 s respectively. Table 2 depicts the total harmonic distortion of two different controllers at different times, we can see the proposed controller has a desired control performance compared with traditional controller. At same time, it is obvious that the proposed controller has an excellent dynamic performance.

Fig. 12 shows the sliding surface waveform under the two control strategies. Although the rang of sliding surface fluctuation using proposed controller is slightly larger than the rang of sliding surface fluctuation using traditional controller, when the non-linear load changes, the waveform of the sliding surface using proposed controller does not change significantly. The waveform of sliding surface using traditional controller will suddenly enlarge, especially when the non-linear load changes, and such phenomenon will increase the switching loss of IGBT in practical applications.

In summary, a dynamic sliding mode control using integral switching gain illustrates has a better compensation performance and robustness compared with traditional SMC though simulation. Meanwhile, the proposed controller can suppress chattering.

VI. HARDWARE IN THE LOOP EXPERIMENT

With the development of microprocessors, digital signal processing (DSP) becomes an important way to verify control algorithm. However, due to processor limits, complex intelligent control algorithms are difficult to achieve ideal results

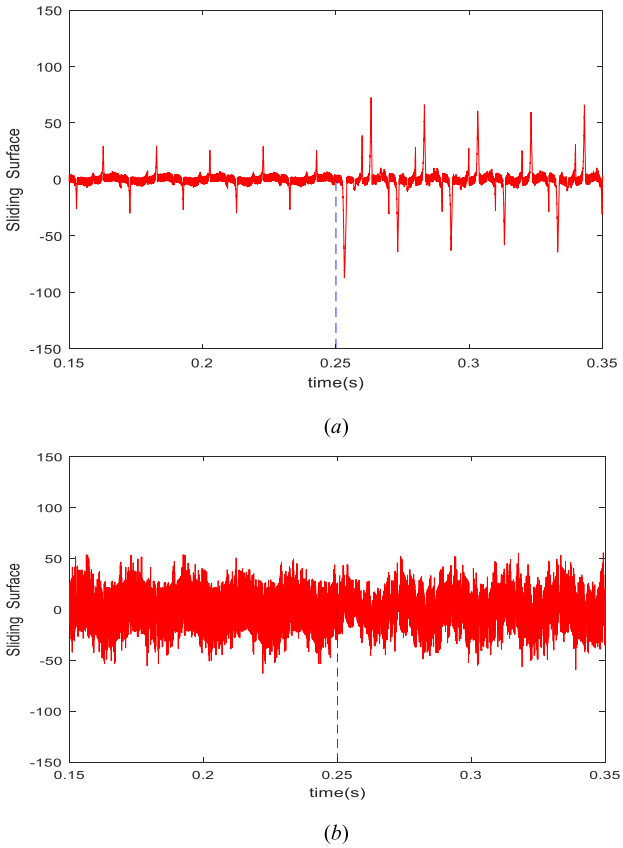

FIGURE 12. Sliding surface waveform (*a*) using traditional controller (*b*) using proposed controller.

on DSP, which makes researchers spend a lot of time on hardware, it is not conducive to the development of control algorithms.

The dSPACE Real-Time system is a new control system development and test platform based on Matlab/Simulink. dSPACE processing speed is faster than DSP, so dSPACE can implement more complex algorithms. Meanwhile, dSPACE can seamlessly connect to simulink, which greatly reduces the development time of control algorithms. In order to verify the actual application effect of the proposed control algorithm, this paper uses DS1104 to design an experimental prototype. Due to site constrains, the experimental prototype adopts low-voltage (24V/50HZ) and single-phase active power filter structures for safety. The design of the experimental prototype based on dSPACE is divided into three steps:

(1) Offline simulation by creating a simulink model. The simulation model established in Section V is the offline simulation model, but the experimental prototype is a single-phase model, we need to modify the original model slightly.

(2) The Real time integration (RTI) library is an important link between dSPACE system and simulink toolbox. Select the corresponding I/O module from the RTI library, and combine the control algorithm module with the offline model. Fig. 13 is the established RTI model.

(3) When the program is downloaded to the DS1104, the Controldesk software is used to design a monitoring

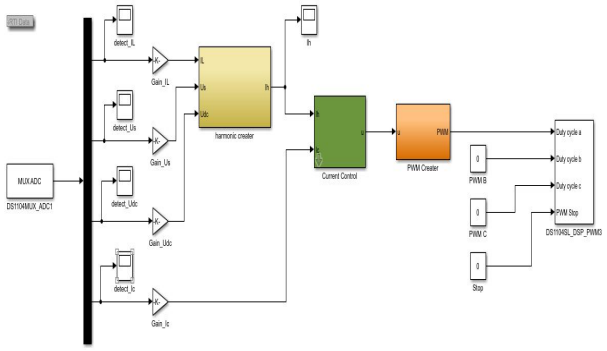

FIGURE 13. Implementation of the control system in the dSPACE.

FIGURE 14. Data monitoring and regulation of the control system in the controldesk.

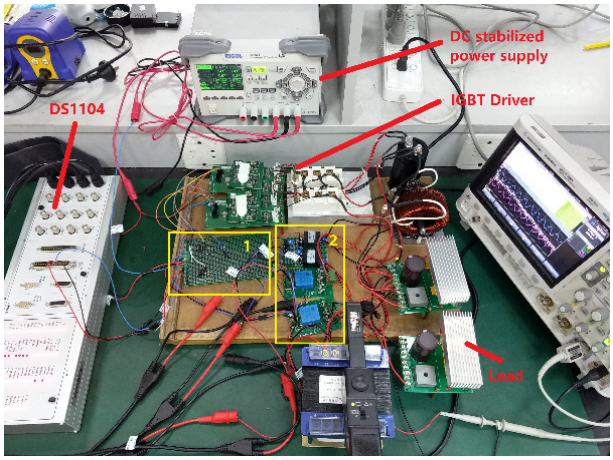

FIGURE 15. Single-phase active power filter prototype.

interface, which can display the state of the acquired data, regulate the parameters of the control algorithm in real time and plot the system response curve.

In the Fig. 13, DS1104MUX_ADC1 module corresponds to the analog input of the DS1104 control platform, DS1104SL_DSP_PWM3 corresponds to the three-phase PWM output of the DS1104 control platform. However, experimental prototype is single-phase structure, we just need

(*a*)

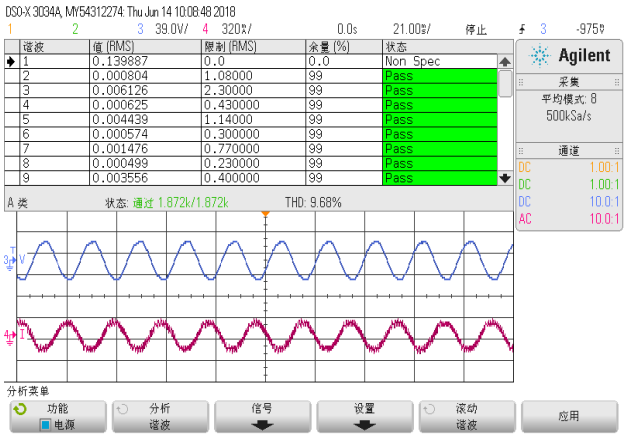

(*b*)

FIGURE 16. FFT of the supply current, supply voltage (blue curve or yellow curve) and supply current (purple curve) (a) before compensation (b) after compensation.

to use one phase PWM output, and the unused PWM output needs to be set to zero. When the RTI model is built, clicking RTI build in simulink to compile, generate and download C code. Fig. 14 is the monitoring interface in the Controldesk, where (a) is the tracking waveform of the instruction reference current, (b) is the capacitor voltage, (c) is the grid voltage.

TABLE 3. The experimental prototype parameters.

Parameters	Values
Single-phase voltage	$24V_{rms}$ / $50Hz$
Non-linear load	$R1 = 5\Omega,\ R2 = 15\Omega$ $C = 1e^{-3}F$
Main circuit parameters	$L = 10e^{-3}H,\ R = 1\Omega$ V_{ref} =50V

Table 3 shows the hardware parameters of the experimental prototype. Table 3 is the relevant parameters for designing the active power filter prototype. Fig. 15 is an experimental prototype, where 1 is the signal amplification module, 2 are voltage and current sensors respectively, the data detected by the sensors is given to the AD interface of the DS1104, the PWM voltage output by DS1104 is consistent with TTL voltage, but the IGBT driver voltage is close to 15V, so we need a voltage amplification module, and the amplification gain is about 2.7.

In the Fig. 16, we can clearly discover that the supply current seriously distorts before compensation, the THD value of supply current measured by the Agilent 3000X series oscilloscope is 34.8%, but when DS1104 goes to online, it means the control algorithm starts to work, the supply current approaches standard sine wave, and the THD value of supply current approach 9.68%.

The experimental results show that the proposed controller has a good compensation effect. Further research will adopt neural network to approximate the nonlinear part of the APF system.

VII. CONCLUSIONS

In this paper, a dynamic sliding mode control with integral switching gain for APF has been put forward, this control strategy combines the advantages of dynamic sliding mode and integral gain. Simulation results illustrate that the proposed control strategy have a better tracking performance, robustness and very low THD value compared with traditional SMC strategy, there is also some achievement in eliminating chattering. Finally, considering the practical application of the proposed algorithm in APF, utilize a rapid prototyping platform (dSPACE DS1104) to verify practicality. Experimental results show that the proposed controller can effectively eliminate chattering and suppress harmonic current.

By contrast, the experimental results are different from the simulation results. The error is mainly caused by the dynamic sliding surface. Therefore, in further research, intelligent algorithm such as neural network and fuzzy control will be used to approximate the unknown error in the control system, and improve the expression of the dynamic sliding surface.

REFERENCES

[1] I. Ranaweera, S. Sanchez, and O. Midtgård, "Residential photovoltaic and battery energy system with grid support functionalities," in *Proc. IEEE 6th Int. Symp. Power Electron. Distrib. Gener. Syst. (PEDG)*, Aachen, Germany, Jun. 2015, pp. 1–7.

[2] B. Singh, K. Al-Haddad, and A. Chandra, "A review of active filters for power quality improvement," *IEEE Trans. Ind. Electron.*, vol. 46, no. 5, pp. 960–971, Oct. 1999.

[3] B. Singh, B. N. Singh, A. Chandra, K. Al-Haddad, A. Pandey, and D. P. Kothari, "A review of three-phase improved power quality AC-DC converters," *IEEE Trans. Ind. Electron.*, vol. 51, no. 3, pp. 641–660, Jun. 2004.

[4] H. Bai, X. Wang, and F. Blaabjerg, "A grid-voltage-sensorless resistive-active power filter with series LC-filter," *IEEE Trans. Power Electron.*, vol. 33, no. 5, pp. 4429–4440, May 2018.

[5] W. U. K. Tareen and S. Mekhielf, "Three-phase transformerless shunt active power filter with reduced switch count for harmonic compensation in grid-connected applications," *IEEE Trans. Power Electron.*, vol. 33, no. 6, pp. 4868–4881, Jun. 2018.

[6] G. Son, H.-J. Kim, and B.-H. Cho, "Improved modulated carrier control with on-time doubler for a single-phase shunt active power filter," *IEEE Trans. Power Electron.*, vol. 33, no. 2, pp. 1715–1723, Feb. 2018.
[7] S. Bosch, J. Staiger, and H. Steinhart, "Predictive current control for an active power filter with LCL-filter," *IEEE Trans. Ind. Electron.*, vol. 65, no. 6, pp. 4943–4952, Jun. 2018.
[8] B. Harshithananda, S. Priyashree, and H. A. Vidya, "Mitigation of harmonics using hysteresis control technique of VSI based active power filter," in *Proc. Int. Conf. Smart Grids, Power Adv. Control Eng. (ICSPACE)*, Bangalore, India, Aug. 2017, pp. 258–261.
[9] P. Yang, C. Tang, Z. Xu, and Y. Zheng, "3-D space vector PWM for three-phase four-wire active filter," in *Proc. 18th Int. Conf. Elect. Mach. Syst. (ICEMS)*, Pattaya, Thailand, Oct. 2015, pp. 616–619.
[10] Z. Tang and D.-F. Liao, "The research and simulation of shunt hybrid active power filter based on PSCAD/EMTDC," in *Proc. Int. Conf. Energy Environ. Technol.*, Guilin, China, Oct. 2009, pp. 352–356.
[11] J. Liu, S. Vazquez, L. Wu, A. Marquez, H. Gao, and L. G. Franquelo, "Extended state observer-based sliding-mode control for three-phase power converters," *IEEE Trans. Ind. Electron.*, vol. 64, no. 1, pp. 22–31, Jan. 2017.
[12] J. Liu, S. Laghrouche, and M. Wack, "Observer-based higher order sliding mode control of power factor in three-phase AC/DC converter for hybrid electric vehicle applications,' *Int. J. Control*, vol. 87, no. 6, pp. 1117–1130, 2014.
[13] S. Saetieo, R. Devaraj, and D. A. Torrey, "The design and implementation of a three-phase active power filter based on sliding mode control," *IEEE Trans. Ind. Appl.*, vol. 31, no. 5, pp. 993–1000, Sep./Oct. 1995.
[14] H. D. Battista and R. J. Mantz, "Harmonic series compensators in power systems: Their control via sliding mode," *IEEE Trans. Control Syst. Technol.*, vol. 8, no. 6, pp. 939–947, Nov. 2000.
[15] G. Zhu, G. Wang, and D. Hua, "Sliding mode control with variable structure of series active power filter," in *Proc. IEEE Power Energy Soc. Gen. Meeting*, Calgary, AB, Canada, Jul. 2009, pp. 1–6.
[16] S. Yarahmadi, G. A. Markade, and J. Soltani, "Current harmonics reduction of non-linear load by using active power filter based on improved sliding mode control," in *Proc. 4th Annu. Int. Power Electron., Drive Syst. Technol. Conf.*, Tehran, Iran, Feb. 2013, pp. 524–528.
[17] J. Fei and T. Wang, "Adaptive fuzzy-neural-network based on rbfnn control for active power filter," *Int. J. Machines Learn. Cybern.*, no. 6, pp. 1–12, 2018, doi: 10.1007/s13042.-018-0792-y.
[18] J. Fei and C. Lu, "Adaptive fractional order sliding mode controller with neural estimator," *J. Franklin Inst.*, vol. 355, no. 5, pp. 2369–2391, 2018.
[19] Y. Chu, J. Fei, and S. Hou, "Dynamic global proportional integral derivative sliding mode control using radial basis function neural compensator for three-phase active power filter," *Trans. Inst. Meas. Control*, vol. 40, no. 12, pp. 3549–3559, 2018.
[20] J. Liu, H. An, Y. Gao, C. Wang, and L. Wu, "Adaptive control of hypersonic flight vehicles with limited angle-of-attack," *IEEE/ASME Trans. Mechatronics*, vol. 23, no. 2, pp. 883–894, Apr. 2018.
[21] G. Sun, L. Wu, Z. Kuang, Z. Ma, and J. Liu, "Practical tracking control of linear motor via fractional-order sliding mode," *Automatica*, vol. 94, pp. 221–235, Aug. 2018.
[22] Y. Zhao, J. Wang, F. Yan, and Y. Shen, "Adaptive sliding mode fault-tolerant control for type-2 fuzzy systems with distributed delays," *Inf. Sci.*, vol. 473, pp. 227–238, Jan. 2019.
[23] S.-G. Jeong and M.-H. Woo, "DSP-based active power filter with predictive current control," *IEEE Trans. Ind. Electron.*, vol. 44, no. 3, pp. 329–336, Jun. 1997.
[24] D. C. Silva, B. F. Musse, N. L. Silva, P. M. de Almeida, and J. G. de Oliveira, "Hardware in the loop simulation of shunt active power filter (SAPF) utilizing RTDS and dSPACE," in *Proc. Brazilian Power Electron. Conf. (COBEP)*, Juiz de Fora, Brazil, Nov. 2017, pp. 1–6.
[25] S. Hou and J. Fei, "Finite-time adaptive fuzzy-neural-network control of active power filter," *IEEE Trans. Power Electron.*, to be published, doi: 10.1109/TPEL.2019.2893618.
[26] M. Popescu, A. Bitoleanu, and V. Suru, "A DSP-based implementation of the p-q theory in active power filtering under nonideal voltage conditions," *IEEE Trans. Ind. Informat.*, vol. 9, no. 2, pp. 880–889, May 2013.

YUN CHEN received the B.S. degree in electrical engineering from Hohai University, China, in 2018, where he is currently pursuing the M.S. degree in electrical engineering. His research interests include power electronics, nonlinear control, and neural networks.

JUNTAO FEI (M'03–SM'14) received the B.S. degree in electrical engineering from the Hefei University of Technology, China, in 1991, the M.S. degree in electrical engineering from the University of Science and Technology of China, in 1998, and the M.S. and Ph.D. degrees in mechanical engineering from The University of Akron, Akron, OH, USA, in 2003 and 2007, respectively. He was a Visiting Scholar with the University of Virginia, Charlottesville, VA, USA, from 2002 to 2003. He was a Postdoctoral Research Fellow, and also an Assistant Professor with the University of Louisiana, Lafayette, LA, USA, from 2007 to 2009. He is currently a Professor with Hohai University, China. His research interests include adaptive control, nonlinear control, intelligent control, dynamics and control of MEMS, and smart materials and structures.